Mechanisms by which extratropical wave forcing in the winter stratosphere induces upwelling in the summer hemisphere

Ka Kit Tung and Jonathan S. Kinnersley

Department of Applied Mathematics, University of Washington, Seattle, Washington

Abstract. Observational evidence presented here suggests that zonal body force in the middle- and high-latitude winter stratosphere can induce an extensive circulation with upwelling spreading into the summer hemisphere. Numerical model results are used to investigate the nature of the circulation anomaly and the mechanism by which it is produced. It is found that nonlinearity is important in allowing cross-equatorial flow, which connects the upwelling in the summer hemisphere to the wave forcing in the winter hemisphere. The connection between the summer and winter hemispheres in our model is through the cross-equatorial flow in the upper stratosphere in a region of low angular momentum gradient. The existence of an extensive circulation and the required cross-equatorial flow is sensitive to the location of the wave forcing in the winter extratropics. It requires that the wave forcing be present between 40 and 60 km and extends equatorward of 30° in the winter stratosphere. In the real atmosphere, planetary waves presumably break predominantly above 40 km and more equatorward in January and February. We therefore expect that such an extensive circulation exists in the atmosphere during late winter. Indeed, our model tracer, temperature, and zonal wind patterns are very similar to those observed with respect to the response of the nearly global circulation to extratropical wave forcing in winter.

1. Introduction

Since the early work of *Brewer* [1949] and *Dobson* [1956], based on observations of the seasonal behavior of stratospheric tracers (water vapor and ozone), a picture emerged of the existence of a stratospheric mean circulation, called the Brewer-Dobson circulation (which is now more precisely defined as the zonal mean circulation along isentropic coordinates, or as a Transformed Eulerian mean [*Andrews et al.*, 1987]). This mean circulation generally subsides in the winter extratropics, with the compensating upwelling located generally in the tropics. The cause of the tropical upwelling is now understood to be nonlocal, being controlled by planetary wave forcing in the extratropical westerly wave guide, the so-called "extratropical wave pump" [*Holton et al.*, 1995]. The focus of the present work is on where in the tropics the upwelling occurs and what mechanism controls its path.

The concept of the existence of upwelling remote from the region of wave forcing is not new. *Holton et al.* [1995] suggest that as planetary waves break or dissi-

pate in the winter extratropical upper stratosphere, the resulting wave drag, which is an easterly momentum body force for the zonal mean flow, would induce a poleward flow in the region of the forcing, and subsidence in the middle and lower stratosphere below it (i.e., "downward control" [*Haynes et al.*, 1991]). It is understood that there would be upwelling remote from the region of forcing to complete the circulation. As pointed out by *McIntyre* [1999], while the "pump" largely controls the net mass flux drawn up from the tropical troposphere, it does not dictate the "pathway" of the upwelling. The latter may be determined by a number of factors: the latitudinal and altitudinal location of the "pump," nonlinearity, and equatorial friction, as we will discuss.

Observational evidence appears to show a time-mean (monthly or seasonal mean) circulation in the stratosphere during solsticial seasons whose upwelling branch spreads to the hemisphere opposite that of the downward branch. Radiative calculations using the observed temperature and distribution of (radiatively active) tracers often show that the upwelling branch of the Brewer-Dobson circulation is confined to the tropics near the tropopause region but broadens to the summer hemisphere higher up in the stratosphere. Near 40 km the upwelling branch during winter extends beyond the tropical latitudes of the opposite hemisphere [see *Rosenlof*, 1995; *Yang et al.*, 1990, Figure 8; *Plumb and Eluszkiewicz*, 1999, Figure 2]. Although there is much uncertainty concerning the accuracy of radiative calculations of net heating in the stratosphere, this upwelling feature is nevertheless likely to be true, as its effect is also manifested in the observed seasonal distribution of stratospheric tracers and other dynamical quantities. (For HALOE water vapor, see *Rosenlof et al.* [1997]; for TOMS ozone, temperature and zonal wind, see section 4).

Since the mean meridional circulation cannot be measured accurately, the evidence thus far is indirect. In addition to this uncertainty, there is also the possibility that the summer hemisphere upwelling may be unrelated to the winter hemisphere wave forcing. We will first attempt to address this last issue with a correlative study. It will be shown that the extensive circulation, or rather the pattern of the distribution of chemical tracers and dynamical variables transported by it, is associated with the extratropical wave drag. Causal relationships cannot be established by the correlative study but can more appropriately be demonstrated in a numerical model. Thus another purpose of the present study is to, with an imposed extratropical wave drag, generate in a numerical model of the middle

atmosphere a meridional circulation and compare the pattern of tracer distributions and dynamical variables in the model with the observed pattern. Having found a favorable comparison, we then examine the diagnostics of the model to isolate the mechanisms responsible for this extensive circulation in the model and to infer their relevance in the real atmosphere.

2. Discussion of the Mechanisms

The mean meridional diabatic circulation, the Brewer-Dobson circulation, is one of the ways the atmosphere responds to body forces imposed in the extratropics of the middle atmosphere. Here we need to make the important distinction between transient and steady state responses. It is well known, both observationally and theoretically, that the transient large-scale response of the atmosphere can be extensive. *Eliassen* [1951] and, more importantly, *Plumb* [1982] and *Garcia* [1987], showed that in the atmosphere's attempt to restore thermal-wind balance upset by externally imposed mechanical driving, a meridional circulation of nearly global extent is generated even when the forcing is restricted to the middle and high latitudes of one hemisphere. In these linear models the geostrophic balance between the mean Coriolis torque and the zonal momentum forcing is broken by the transient acceleration of the zonal wind. At steady state however, these transient circulations collapse to the region of forcing, unless friction, which can also break the geostrophic constraint, is present. It is not clear that in the atmosphere, Rossby wave drag behaves frictionally, since its action does not appear to be a restoring one. While inertial instability in the equatorial stratosphere may act as a relaxational friction near the equator, it is more difficult to justify a uniform friction present globally [*Semeniuk*, 2000; *Semeniuk and Shepherd*, 2001]. In the absence of friction away from the region of forcing, the time-mean meridional circulation in most cases should be confined to the hemisphere of the forcing, if the latter is located in the extratropics [*Plumb and Eluszkiewicz*, 1999].

We now turn our attention to steady or time-mean circulation. Under geostrophy, which should hold away from the equator, the zonal mean diabatic circulation $(\overline{v}, \overline{w})$, where the overhead bar denotes zonal average (either defined as the transformed Eulerian zonal mean or the zonal mean on isentropic surfaces), is governed by the zonal mean zonal momentum equation,

$$-f\overline{v} = F, \tag{1}$$

where F is the wave forcing (more precisely, the Eliassen-

Palm divergence), and the continuity equation,

$$\frac{\partial}{\partial y}(\rho_0 \overline{v}) + \frac{\partial}{\partial z}(\rho_0 \overline{w}) = 0. \qquad (2)$$

In a region of planetary wave drag (the so-called "surf zone") ($F < 0$), $f\overline{v}$ is positive and the flow is therefore poleward. Outside the region of wave drag, $\overline{v} = 0$. The circulation must be completed by upwelling ($\overline{w} > 0$, with $\rho_0 \overline{w} = \text{const}$) on the equatorial edge of the surf zone and subsidence ($\overline{w} < 0$) on the poleward edge (see Figure 1, from Figure 1(a) of *Plumb and Eluszkiewicz* [1999]). Therefore if we assume that the surf zone does not extend into the tropics, it is difficult to explain the existence of upwelling over the tropics, let alone over the opposite hemisphere. *Plumb and Eluszkiewicz* [1999] pointed out that in order to have upwelling over the tropics, with its implied cross-equatorial meridional flow, equation (1) must fail. It can fail if either (1) the flow is fundamentally nonlinear or (2) there exists a region over the equator where friction is important. *Plumb and Eluszkiewicz* [1999] suggested the second possibility, since they found that their model behaves linearly in the lower stratosphere, where most of the mass flux occurs. In the upper stratosphere of their model, however, the flow shows clear signs of nonlinearity, as pointed out by the authors.

Figure 1

The inclusion of a small Rayleigh friction allows the upwelling region in the Plumb and Eluszkiewicz linear model to extend from the edge of the surf zone to over the tropics, provided that the surf zone extends to within a frictional boundary layer centered at the equator. The width of that boundary layer is given by $L_R P^{1/4}$, where L_R is the equatorial Rossby radius and P is the ratio of frictional to radiative damping rates. Plumb and Eluszkiewicz estimated that this frictional region, where flows can cross angular momentum contours, occurs within $\sim \pm 8^\circ$ of the equator. In the model of *Semeniuk and Shepherd* [2001] this viscous layer is within $\pm 6^\circ$ of the equator. This mechanism may be responsible for the tropical upweling in the lower stratosphere. Another possibility is the presence of wave body force in the tropical region. *Sankey* [1998] estimated that a small magnitude of 1.23 m^{-1} d^{-1} of wave forcing in the tropics can produce the observed magnitude of tropical upwelling, but he found that the time-averaged forcing close to the equator in the United Kingdom Meteorological Office data is not this large. Nevertheless, given the uncertainty regarding wave forcing in the tropical region, this mechanism cannot be dismissed. We now turn our attention to a feature of the circulation not explained by either of the two mechanisms mentioned above.

As pointed out by Plumb and Eluszkiewicz, there is no bias toward the opposite hemisphere for the upwelling branch of the circulation in a linear frictional model. Nonlinear models are known to be capable of producing such a bias in solstitial seasons when there is a gradient at the equator of the radiative equilibrium temperature. Nonlinear circulations can exist in the tropics even without wave driving, but they are normally confined to within $\pm 30^\circ$ of the equator if the radiative equilibrium temperature is symmetric about the equator (see *Held and Hou* [1980] for the tropospheric case). Upwelling occurs over the equator and subsidence over the subtropics in both hemispheres, forming two cells. During solstitial seasons, when there is a nonzero gradient of radiative equilibrium temperature at the equator, the winter cell is greatly strengthened in both strength and meridional extent. The location of the upwelling branch of the winter cell is biased toward the summer hemisphere (see *Lindzen and Hou* [1988], *Fang and Tung* [1999] for the tropospheric Hadley circulation, and *Dunkerton* [1989] for the stratospheric case). *Jones et al.* [1998] and *Kinnersley* [1999] showed that even the equatorial Quasi-Biennial Oscillation should be associated with an asymmetrical (one wintercell) meridional circulation during solstice. In the absence of explicit wave drag, the presence of moderate friction in the winter extratropics strengthens the winter cell and extends it to the midlatitudes in the winter hemisphere, accompanied by an upwelling extending into the summer hemisphere [*Dunkerton*, 1989; 1991; *Kinnersley*, 1999]. Using an equal-area rule, *Dunkerton* [1989] argued that the presence of wave drag in the winter hemisphere should further strengthen the circulation, though no explicit wave driving was considered in either *Dunkerton* [1989] or *Kinnersley* [1999]. This will be considered in the present work. See also the Ph.D thesis of *Semeniuk* [2000] and of *Sankey* [1998].

The latitudinal and altitudinal location of the wave drag appears to be an important factor in determining the meridional extent of the circulation. If the extratropical wave drag does not intrude into the subtropics, the wave-driven circulation exists in the extratropics, and its meridional extent is confined to the extent of the forcing. In the equatorial region, there exists an independent nonlinear Hadley-type circulation, which is asymmetrical with respect to hemispheres during the solstice season. In the solstitial season, the downward branch of the tropical winter cell may overlap with that of the wave driven cell in the winter hemisphere. The question is: Is this a simple superposition, or will the tropical upwelling be intensified and moved partly to

the summer hemisphere? We will show that the latter is the case under some conditions in our model.

If part of the upwelling branch occurs in the hemisphere opposite to the hemisphere of the "wave pump," some streamlines must cross the equator. Air can cross the equator either if there is friction (as is the case of Plumb and Eluszkiewicz, also probably the case in the lower stratosphere) or if there exists a region of low angular momentum gradient over the equator [*Dunkerton*, 1989]. For an upwelling flow, which brings mass from the lower to the upper stratosphere, the effect of nonlinearity, in the form of angular momentum advection neglected in equation (1), becomes more important the higher up the circulation extends. It is limited from above by a region where significant gravity wave breaking alters the momentum balance from nonlinear to frictional. This frictional level occurs above 60 km in our model. The region below 60 km, from 45 km to (almost) 60 km, is dominated by nonlinearity in the tropical region, where the angular momentum gradient is greatly reduced. The situation we have in mind for the upper stratosphere is more like that depicted in part (a) of Plate 1, which is from our numerical model (to be discussed more later), than in Figure 1. This allows cross-equatorial meridional flow, which connects the upwelling in the lower stratosphere in the summer hemisphere to the region of planetary wave breaking in the winter extratropics, where the balance implied by equation (1) again holds. This "sideways control" of the wave pump was previously suggested by *Dunkerton* [1989]. The extension of the upwelling branch into the summer hemisphere below the stratopause is a function of the shape of the angular momentum contours. In the region of no forcing, $F = 0$, the circulation streamlines follow approximately the angular momentum contours. So if one examines a cross-equatorial streamline in the upper stratospheric nonlinear region, which connects to the wave forcing region in the winter extratropics, and traces it backward along the angular momentum contour, one will find that a part of the upwelling branch originates from the summer hemisphere in the lower stratosphere. This is a consequence of the equatorward and upward slope of the angular momentum contour as it changes from almost vertical in the lower stratosphere to tilting toward the equator in the upper stratosphere (see Plate 1a).

Plate 1

In the nonlinear numerical model of Plumb and Eluszkiewicz the placement of a rigid lid at 60 km and a sponge layer between 55 and 60 km induces a reverse flow (from winter to summer hemisphere) in that region. The nonlinear cross-equatorial flow (from summer

to winter hemisphere) occurs lower down, at around 40 km (see their Figure 5). Tracing the angular momentum contours downward from a cross-equatorial streamline near 40 km leads also to the summer hemisphere for a portion of the upwelling branch in the lower stratosphere, but it is located much closer to the equator than in our case. Whether in the real atmosphere the gravity-wave-dominated frictional layer occurs above or below 60 km is an open question. Comparison of model results with the observed tracer patterns thus becomes useful.

In section 3 we will briefly describe our nonlinear numerical model. More importantly, we will attempt to establish its ability to simulate the extent of the upwelling region in the real atmosphere by comparing model results with the observed patterns. This is done in section 4. In section 5, the various control experiments are explained, and conclusion is drawn in section 6.

3. Model

The model used in this study has been extensively documented by *Kinnersley* [1996]. It has been used to study interannual variability of the stratospheric zonal wind and ozone caused by the variability in the planetary wave amplitudes from the lower atmosphere, and by the different phases of the equatorial QBO [*Kinnersley*, 1998; *Kinnersley and Tung*, 1998]. Comparison with the observed interannual variability was done by *Kinnersley and Tung* [1998] and was found to be rather satisfactory, with high correlations between the model and observed patterns. The full set of governing equations can be found in the works of *Kinnersley and Harwood* [1993], *Tung* [1986], and *Yang et al.* [1991]. Here we list only the most important one, for the purpose of later discussions:

$$\frac{\partial}{\partial t}\overline{L} + \overline{v}\frac{\partial}{\partial y}\overline{L} + \overline{w}\frac{\partial}{\partial z}\overline{L} = F\cos\varphi, \qquad (3)$$

where $\overline{L} = [\overline{u} + \Omega a\cos\varphi]\cos\varphi$ is the zonal mean angular momentum per unit mass. F is the Ertel potential vorticity flux ("wave drag"). $y \equiv a\sin\varphi$. Equation (1) is the geostrophic approximation of (3), since at mid-latitudes, $\frac{\partial}{\partial y}\overline{L} \cong 2\Omega\sin\varphi = f$.

Although the model is three-dimensional (3D), involving the interaction of zonal averages and three longest planetary waves, here only the zonal-mean quantities are calculated. The required wave forcing, in the form of potential vorticity flux, is obtained from the stored values of previous 3-D runs. The values of PV flux, calculated for the period from March 1980 to February 1993, are averaged and used as the "climatological" base control. The model is formulated in isentropic coordinates.

It has 19 horizontal boxes from pole to pole and 29 levels in the vertical, from the ground to about 100 km. The zonal mean radiation, chemistry, and dynamics in the model are interactive with the zonal mean dynamics and the zonal mean transport of the tracers needed for the chemistry and radiation modules. Perturbation experiments are conducted by artificially enhancing by 20% the stored planetary wave potential vorticity flux of the base control in different latitudinal bands and at different heights. (The resulting PV flux turns out to be negative.) The perturbation experiments we will present can be viewed as perturbations due to increased planetary wave drag (negative zonal body force). The anomaly pattern produced will be different for a different location of this perturbation wave drag. We are more interested in the patterns produced and in isolating the mechanisms responsible for these patterns than in simulating the actual magnitude of the interannual variability in the stratosphere.

Above about 60 km the model includes a frictional parameterization of gravity wave drag. In general, an enhancement of the planetary wave PV flux leads to a decrease in stratospheric and mesospheric winter jet which, above 60 km, leads to a westerly increase in the body force of the zonal wind. We will, however, concentrate on the region below 60 km.

The four perturbation experiments involve enhancing by 20% the stored PV flux calculated in the base control run in certain regions:

Experiment I	20% enhancement of PV flux everywhere north of the northern *subtropics* and for all heights;
Experiment II	20% enhancement of PV flux everywhere in the northern *extratropics* and for all heights;
Experiment III	same as Experiment I except the enhancement is applied only *below* about 42 km;
Experiment IV	same as Experiment I except the enhancement is applied only *above* about 42 km.

Our model grid points are spaced 9° of latitude apart. There is a grid point at the equator. The next grid point is at 9°, and then 18, 27°, etc. In Experiment I the enhancement of PV flux is applied in the third grid point in the Northern Hemisphere and all the grid points north of it. In Experiment II the enhancement of PV flux is applied in the fourth grid point in the Northern Hemisphere and all the grid points north of it. "Perturbation" or "anomalous" quantities are obtained by subtracting the climatological values from the results of these experiments (with 20% PV flux enhancements).

4. Comparison With Observation

For the purpose of comparing with our numerical results, we first attempt to infer the observed pattern of the anomalous circulation caused by an anomaly in the wave body force in the extratropics in winter stratosphere. The "anomaly" in the observed data is from the observed interannual variability as deviations from the climatological mean. The wave body force (the Eliassen-Palm flux divergence (or equivalently the potential vorticity flux in isentropic coordinates)) is difficult to calculate accurately from the observed data due to the high spatial derivatives involved. Instead a proxy index is used. This index, called NZWA (for northern zonal wind acceleration), is obtained by averaging the monthly mean zonal wind acceleration over the latitude range of 50°N-90°N and presure range of 30-10 mbar. (Although the index uses data only below 10 mbar, it should also represent the wave forcing throughout the stratosphere because of the vertical coherence of the rate of change of the zonal wind in the stratosphere.) The global distribution of the *rates of change* of Total Ozone Mapping Spectrometer (TOMS) and Solar Backscatter Ultraviolet Spectrometer (SBUV) ozone, Halogen Occulation Experiment (HALOE) methane, National Centers for Environmental Prediction (NCEP) temperature and zonal wind distribution are correlated against this NZWA index. The regressed quantities are obtained by multiplying the correlation coefficient by the standard deviation. These can be interpred as the patterns "caused by" or "due to" the extratropical wave forcing in the winter stratosphere. The reason the *rate of change* of a tracer concentration is used instead of the concentration itself is because we are interested in the meridional circulation patterns which, although cannot be measured directly, influences the rates of change of tracers advected by it. Specifically, the tracer transport equation is

$$\frac{\partial}{\partial t}\overline{\chi} = -\overline{v}\frac{\partial}{\partial y}\overline{\chi} - \overline{w}\frac{\partial}{\partial z}\overline{\chi} + \overline{P},$$

where $(\overline{v}, \overline{w})$ is the mean (either isentropic mean or transformed Eulerian mean) circulation we are interested in, $\overline{P}$ is the chemical net production rate plus the eddy diffusive transport. It is seen that $(\overline{v}, \overline{w})$ is proportional to the rate of change of the mean tracer mixing ratio $\frac{\partial}{\partial t}\overline{\chi}$, similarly for temperature and zonal wind fields.

Figure 2 shows the regressed anomaly in the rates of change of column ozone from TOMS, as compared with the negative of the anomaly in the rates of change of column ozone produced in the model in Experiment I. The

Figure 2

column density of ozone measures mainly the amount of ozone in the stratosphere. The vertical distribution of ozone is such that an upwelling circulation brings up air low in ozone concentration and thus reduces the column density. In Figure 2, because the negatives are shown, a positive value suggests upwelling, while a negative value indicates subsidence, in the lower stratosphere. It is seen that the model pattern is surprisingly good when compared with the observed pattern. Similar comparisons are done in Plate 2 for temperature (Plate 2a: the observed temperature pattern, and Plate 2b: the modeled pattern) and zonal wind (Plate 2c: the observed zonal wind pattern, and Plate 2d: the modeled pattern). Again, the patterns produced by our model are very similar to the observed, if one does not pay too much attention to the variation in amplitude in the vertical, since Experiment I has only a constant percentage enhancement in the vertical.

Plate 2

In addition to establishing the credibility of the model, these figures can also be taken to show that there exists in both the atmosphere and in our model an extensive meridional circulation affecting tracers and dynamical quantities, with the upwelling branch extending broadly into the tropics and even into the summer (southern) hemisphere. Furthermore, because of the way the experiment is constructed, this circulation is caused by the extratropical wave forcing F. The observed pattern is also probably "caused" by the extratropical wave drag because of its similarity to the model, but strictly speaking no cause and effect has been established by the correlative study of the observed data.

5. Model Diagnostics

5.1. Experiment I, Seasonal Cycle Version

Plate 1a, shown earlier, displays the perturbation meridional circulation velocity arrows overlaid on the contours of the angular momentum from January of Experiment I run through a periodic seasonal cycle. It shows subsidence at high northern latitudes and poleward flow caused by the negative PV flux anomaly. The connection to the summer hemisphere is through cross-equatorial flow across a region of low angular momentum gradient. This region is centered around 50 km but is broadly distributed in height. The angular momentum contours in the summer hemisphere lower stratosphere are almost vertical. They, however, bend toward the equator as they go up, with the bend becoming most severe near 52 km, where it is closest to the equator. It is here that nonlinearity is most important. Above around 55 km, the streamline crosses angular momen-

tum contours, indicating the importance of friction due to the gravity wave drag in the model. Below 52 km, the streamlines generally follow the angular momentum contours but not perfectly so. This is mostly due to the effect of transience and friction as discussed below.

The zonal mean angular momentum equation is given in equation (3). In Plate 3, we show the various terms in the zonal angular momentum budget (divided by $\cos\varphi$): the rate of change of zonal wind due to (Plate 3a) wave body force, (Plate 3b) horizontal advection of angular momentum, (Plate 3c) vertical advection, and (Plate 3d) total circulation (sum of (b) and (c)). Note that the wave body force is not completely balanced by the advection of angular momentum, implying that transience and, possibly, friction are relatively important, contributing up to about 20% of the angular momentum budget.

Plate 3

5.2. Experiment I, Perpetual January Run

To test the idea that nonlinearity might play a significant role in the creation of a cross-equatorial flow in the upper stratosphere (below the region of parameterized gravity wave drag), the model was run again under perpetual January conditions for 3 years. An almost steady state was reached after about 6 months. The effect of transience is eliminated as a cause this way.

All sources and sinks of angular momentum were set to zero within one model box of the equator (within approximately 13.5°N and S of the equator) and below 60 km. This way the explicit friction is eliminated as a term in angular momentum budget. Numerical friction, however, cannot be neglected, but is found later to be small.

If a meridional circulation exists both near and across the equator in this model run then nonlinearity must be playing a role, since in the absence of zonal body force the only way the stratosphere can maintain a steady state is for the advection of angular momentum by the vertical and horizontal components of the circulation to balance, a signature of a nonlinear angular momentum conserving circulation.

In Plate 3(e)—(3h) we show the model diagnostics for this steady state. It shows that the flow is nearly angular momentum conserving in the tropics in the region where wave PV flux and explicit friction were set to zero.

The model zonal wind $\overline{u}$, meridional wind $\overline{v}$ and vertical velocity $\overline{w}$ are shown in Plate 4. Because of their smaller magnitudes, the lower stratospheric velocities are not shown well in Plate 4. Therefore we show separately, in Figure 3, the vertical velocities at 15, 20,

Plate 4

Figure 3

and 25 km. We focus our attention below 60 km in Plate 4 and Figure 3. These figures show that the upwelling is confined to $\pm 30^\circ$ of the equator below 18 km. At 15 km there is a strong peak in upwelling located in the summer (southern) subtropics and in subsidence in the winter (northern) subtropics. This circulation anomaly pattern is similar to the one-cell Hadley circulation pattern in the troposphere during winter. Apparently, the specified PV enhancement strengthens the existing Hadley circulation in the troposphere. Since tropospheric circulation is not the subject of the present study, we shall now turn our attention to the stratosphere. In the lower stratosphere (20 and 25 km) in Figure 3, the peak upwelling is located near the equatorial flank of the anomaly forcing region in the winter hemisphere, consistent with geostrophy. However, the upwelling region increasingly broadened into the summer hemisphere with height. Peak upwelling shifts to the summer hemisphere above 30 km (Plate 4). The cross-equatorial velocity peaks near 50 km, as discussed previously. The zonal wind departs significantly from geostrophy (and hence linearity) in the upper stratosphere.

The circulation velocity vectors are superimposed on the angular momentum contours in Plate 1b, which is quite similar to Plate 1a (and therefore one can infer that the mechanisms we are discussing in the perpetual January run are also likely to be the dominant mechanisms in the seasonal run), and shows cross-equatorial flow most significantly near where the angular momentum gradient is the smallest. By tracing these cross-equatorial streamlines backward (downward and southward), one finds that the upwelling branch originates from the Southern Hemisphere and extends slightly beyond (to the south of) 30°S at 25 km. The decrease in the length of the velocity vectors with decreasing height is due to the fact that in the absence of sources and sinks, $\rho_0 \overline{w}$, the mass flux, is approximately constant. Therefore the velocity itself decreases exponentially, e-folding in each scale height, as density increases.

Incidentally, note the small horizontal gradient and the large vertical gradients of angular momentum in the tropical upper stratosphere. This feature increases the impact of the vertical advection (which is generally downgradient both above and below 50 km), and decreases the impact of the meridional advection, allowing the momentum budget to be balanced in the presence of a significant horizontal velocity. By mass continuity the vertical velocity of the upwelling branch, which is quite weak, spreads over a broad latitude band in the summer hemisphere.

5.3. Sensitivity to the Location of PV Flux Perturbations

The existence of this extensive circulation is sensitive to the location of the wave PV flux perturbations. If the PV flux perturbation occurs too low in the winter stratosphere, it cannot be effectively connected to the summer hemisphere because the connection occurs mainly near 50 km. In this case, the induced circulation is confined to the winter hemisphere, with a bias in its upwelling to the winter subtropics. Plate 5 compares the meridional and vertical velocities in Experiment I, with Experiment III, where the PV flux perturbation is applied only below 42 km and with Experiment IV, where it is applied only above 42 km. Experiment IV captures the nearly global nature of the circulation which is in Experiment I, showing that it is the wave forcing above 40 km which matters. The induced circulation in Experiment III (with wave forcing only below 42 km), on the other hand, appears to be confined to the Northern Hemisphere. (Attention should be focused on the pattern and not on the magnitudes, because a 20% increase in the upper stratospheric PV is larger than a similar percentage increase in PV below 42 km.) Experiment III shows further that the lower stratospheric circulation has the linear characteristics predicted by Plumb and Eluszkiewicz, with the peak upwelling occurring in the winter hemisphere, in the equatorial flank of the forcing. Experiment IV, on the other hand, shows that the upper stratospheric circulation has its upwelling maximum broadened and extended into the summer hemisphere, a nonlinear feature.

Plate 5

The extensive nature of the induced circulation is also sensitive to the latitudinal location of the wave PV flux perturbation. If the wave PV flux perturbation is placed only in the extratropics (Experiment II, Plate 5), geostrophy (equation (1)) applies, and so the induced upwelling occurs in the winter subtropics on the equatorial flank of the surf zone and decays rapidly closer to the equator (see Plate 5, Experiment II near 40 km). Near 45 km there is a separate tropical upwelling centered at the equator and confined to the tropics. In the real atmosphere, the situation in January/February is more similar to Experiment I than Experiment II.

The finding, the sensitivity to the latitudinal extent of the wave forcing, is consistent with that of Plumb and Eluszkiewicz, although our upwelling branch extends farther into the summer hemisphere, because of the effect of stronger nonlinearity discussed earlier.

6. Conclusion

A main objective of the present work is to explain the observed upwelling pathway and the meridional extent of the mean circulation associated with the "extratropical wave pump" at seasonal timescales. The observational evidence presented here, although indirect, seems to support an extensive circulation in the stratosphere with the upwelling branch over the tropics and extending into the summer hemisphere. This picture is not consistent with geostrophic balance between the meridional circulation and the extratropical wave drag. It is, however, consistent with a picture of a nonlinear (nongeosptrophic) circulation induced by the high location of wave drag (above 40 km) and sideways control near the tropical stratopause. A plausible scenario is as follows:

Planetary waves propagate up from the lower atmosphere into the stratosphere in a westerly waveguide located in the extratropics of the winter hemisphere. A planetary wave grows in amplitude with height due to the fact that the environmental density decreases exponentially with height. At some level the wave "breaks" and dissipates, producing easterly body forces acting on the zonal angular momentum. This "breaking" level probably occurs significantly near 40 km and above. The resulting zonal body force induces a poleward flow in the region of the body force and subsidence below the level of forcing. If the region of wave forcing is confined to the extratropics, then the poleward flow terminates at the equatorial flank of the region, as demanded by geostrophy (see Figure 1). Mass is supplied through upwelling in the winter side of the equator, near the equatorial flank of the "surf zone." As pointed out by Plumb and Eluszkiewicz, there then cannot be any upwelling throughout the tropics, unlike the case in the real atmosphere. Such kind of extratropical wave forcing is not effective in inducing the extensive circulation which is inferred here from observation of tracer distribution and dynamical fields.

In late winter (January and February for the northern winter),the surf zone probably intrudes more equatorward in the upper stratosphere. Then it can connect with a cross-equatorial flow from the summer hemisphere. The pathway for this "sideways control" occurs probably near 50 km where the angular momentum gradient is weakest. Contours of constant angular momentum in the summer hemisphere slopes with height, being almost vertical in the lower stratosphere and tilting toward the equator as height increases up to the stratopause. In the absence of body forces in the summer stratosphere, the circulation mass stream-

line follows an angular momentum contour. The cross-equatorial flow at 50 km can be traced approximately to its origin in the lower stratosphere in the summer hemisphere along these angular momentum contours. The complete circulation cell then becomes extensive, with upwelling extending slightly beyond 30° of latitude in the summer hemisphere. The observed behavior of ozone from TOMS ozone, HALOE water vapor [*Rosenlof*, 1997] and the radiative calculations of net heating in the lower stratosphere [*Rosenlof*, 1995; *Yang et al*, 1990; *Plumb and Eluszkiewicz*, 1999] is consistent with the existence of such an extensive circulation, with an upwelling extending into the summer hemisphere.

Since circulation mass streamlines deviate from angular momentum contours where wave mixing is important, we do not expect the upwelling branch in the summer midlatitudes to extend into the troposphere. In our model the upwelling branch near 15 km is confined to ±30° of the equator, and broadens into the summer hemisphere only above 20 km.

Acknowledgments. The research was supported by National Science Foundation, Climate Dynamics Program, under ATM9813770. We also benefited from helpful suggestions by anonymous reviewers.

References

Andrewss, D. G., J. R. Holton, and C. B. Leovy, *Middle Atmosphere Dynamics*, Academic Press, 489 pages, 1987.

Brewer, A. W., Envidence for a world circulation provided by the measurements of helium and water vapor distribution in the stratosphere, *Q. J. R. Meteorol. Soc.*, 75, 351-363, 1949.

Dobson, G. M. B., Origin and distribution of the polyatomic molecules in the atmosphere, *Proc. R. Soc. London, Ser. A*, 236, 187–193, 1956.

Dunkerton, T. J., Nonlinear Hadley circulation driven by asymmetric differential heating, *J. Atmos. Sci.*, 46, 956–974, 1989.

Dunkerton, T. J., Nonlinear propagation of zonal winds in an atmosphere with Newtonian cooling and equatorial wavedriving, *J. Atmos. Sci.*, 48, 236–263, 1991.

Eliassen, A., Slow thermally or frictionally controlled meridional circulation in a circular vortex. *Astrophys. Norvegica*, 5(2), 19-60, 1951.

Fang, M., and K. K. Tung, Time-dependent nonlinear Hadley circulation, *J.Atmos. Sci.*, 56, 1797–1807, 1999.

Garcia, R. R., On the mean meridional circulation of the middle atmosphere, *J. Atmos. Sci.*, 44, 3599–3609, 1987.

Haynes, P. H. C. J. Marks, M. E. McIntyre, T. G. Shepherd, and K. P. Shine, On the "downward control" of extratropical diabatic circulations by eddy-induced mean zonal forces, *J. Atmos. Sci.*, 48, 651–678, 1991.

Holton, J. R., P. H. Haynes, M. E. McIntyre, A. R. Douglass, R. B. Rood, and L. Pfister, Stratosphere-troposphere exchange, *Rev. Geophys.*, 33, 403–439, 1995.

Jones, D. B. A., H. R. Schneider, and M. B. McElroy, Effects of quasi-biennial oscillation on the zonally averaged transport of tracers, *J. Geophys. Res.*, 103, 11235–11249, 1998.

Kinnersley, J. S., The climatology of the stratospheric "THIN AIR" model, *Quart. J. Roy. Meteor. Soc.*, 122, 219–252, 1996.

Kinnersley, J. S., Seasonal asymmetry of the low- and middle-latitude QBO circulation anomaly, *J. Atmos. Sci.*, 56, 1140–1153, 1999.

Kinnersley, J. S. and R. S. Harwood, An isentropic two-dimensional model with an interactive parameterization of dynamical and chemical planetary-wave fluxes, *Q. J. R. Meteor. Soc.*, 119, 1167–1193, 1993.

Kinnersley, J. S. and K. K. Tung, Modeling the interannual variability of ozone due to the equatorial QBO and to extratropical planetary wave variability, *J.Atmos. Sci.*, 55, 1417–1428, 1998.

Lindzen, R. S. and A. Y. Hou, 1988: Hadley circulation for zonally averaged heating centered off the equator, *J. Atmos. Sci.*, 45, 2416–2427, 1988.

Held, I. M. and A. Y. Hou, Nonlinear axially symmetric circulations in a nearly inviscid atmosphere, *J. Atmos. Sci.*, 37, 515–533, 1980.

McIntyre, M. E., How far have we come in understanding the dynamics of the middle atmosphere?, *Proceedings of the 14th European Space Symposium on European Rocket and Balloon Programmes and Related Research, ESA Spec. Pap–437*, edited by B. Kaldeich-Schurmann, Euro Space Aigency Publications Division, ESTEC, Noordwijk, Netherlands, 1999.

Plumb, R. A., Zonally-symmetric Hough modes and meridional circulations in the middle atmosphere, *J. Atmos. Sci.*, 39, 983–991, 1982.

Plumb, R. A. and J. Eluszkiewicz, The Brewer-Dobson circulation: dynamics of the tropical upwelling, *J. Atmos. Sci.*, 56, 868–890, 1999.

Rosenlof, K. H., Seasonal cycle of residual mean meridional circulation in the stratosphere, *J. Geophy. Res.*, 100, 5173–5191, 1995.

Rosenlof, K. H., A. F. Tuck, K. K. Kelley, J. M. Russell, III, and M. P. McCommick, Hemisphere asymmetrics in water vapor and inferences about transport in the lower stratosphere, *J. Geophys. Res.*, 102, 13212–13234, 1997.

Sankey, D., Dynamics of upwelling in the equatorial lower stratosphere, Ph.D. thesis, Cambridge Univ., Cambridge, U.K., 1998.

Semeniuk, K., Mean meridional circulations in the middle atmosphere, PhD thesis, Univ. of Toronto, Toronto, Canada, 2000.

Semeniuk, K. and T. G. Shepherd, Mechanisms for tropical upwelling in the stratosphere, *J. Atmos. Sci.*, in press, 2001.

Tung, K. K., Nongeostrophic theory of zonally averaged circulation, Part I: Formulation, *J. Atmos. Sci.*, 43, 2600–2610, 1986.

Yang, H., K. K. Tung and E. Olaguer, Nongeostrophic theory of zonally averaged circulation, Part II: Eliassen-Palm flux divergence and isentropic mixing coefficient, *J. Atmos. Sci.*, 47, 215–241, 1990.

Yang, H., E. Olaguer, and K. K. Tung, Simulation of the present-day atmospheric ozone, odd nitrogen, chlorine

and other species using a coupled 2-D model in isentropic coordinates, *J. Atmos. Sci.*, 48, 442–471, 1991.

K. K. Tung and J. S. Kinnersley, Department of Applied Mathematics, University of Washington, Seattle, Washington 98195-2420. (email: tung@amath.washington.edu.)

(Received August 25, 2000; revised March 20, 2001; accepted April 25, 2001.)

Paper number 2001JD900228.
0148-0227/01/2001JD900228$09.00

Figure 1. Schematic of the steady meridional circulation produced by midlatitude wave drag, which is confined to the winter midlatitude surf zone and denoted by the shading. Thin lines show contours of angular momentum, assumed here to be dominated by the planetary term in the extratropics. Arrows depict the circulation. (Redrawn from Figure 1a of *Plumb and Eluszkiewicz* [1999] for the case of linear balance of our equation (1).)

Figure 1. Schematic of the steady meridional circulation produced by midlatitude wave drag, which is confined to the winter midlatitude surf zone and denoted by the shading. Thin lines show contours of angular momentum, assumed here to be dominated by the planetary term in the extratropics. Arrows depict the circulation. (Redrawn from Figure 1a of *Plumb and Eluszkiewicz* [1999] for the case of linear balance of our equation (1).)

Plate 1. Perturbation circulation produced by middle- and high-latitude drag in our model (Experiment I, discussed in section 3). Arrows depict anomaly velocity vectors of $(\overline{v}, \overline{w})$. Contours show lines of constant angular momentum, which are also calculated by the model. (a) Seasonal run, (b) perpetual January run.

Plate 1. Perturbation circulation produced by middle- and high-latitude drag in our model (Experiment I, discussed in section 3). Arrows depict anomaly velocity vectors of $(\overline{v}, \overline{w})$. Contours show lines of constant angular momentum, which are also calculated by the model. (a) Seasonal run, (b) perpetual January run.

Figure 2. Negative of the anomaly in the rate of change of ozone column in January/February in the model (Experiment I) and in the regressed TOMS data.

Figure 2. Negative of the anomaly in the rate of change of ozone column in January/February in the model (Experiment I) and in the regressed TOMS data.

Plate 2. Comparison of the January/February values of (a) the observed anomaly (regressed rate of change of zonal mean temperature against NZWA), and (b) the negative of the modeled anomaly in the rate of change of zonal mean temperature in the model (Experiment I). Both are multiplied by the cosine of latitude to emphasize the tropics, (c) observed anomaly for the rate of change of the mean zonal wind, similar to Plate 2a, (d) modeled anomaly of the rate of change of the mean zonal wind, similar to Plate 2b.

Plate 2. Comparison of the January/February values of (a) the observed anomaly (regressed rate of change of zonal mean temperature against NZWA), and (b) the negative of the modeled anomaly in the rate of change of zonal mean temperature in the model (Experiment I). Both are multiplied by the cosine of latitude to emphasize the tropics, (c) observed anomaly for the rate of change of the mean zonal wind, similar to Plate 2a, (d) modeled anomaly of the rate of change of the mean zonal wind, similar to Plate 2b.

Plate 3. Model angular momentum budget in seasonally varying run, showing the rate of change of zonal mean zonal wind due to (a) wave body force, (b) horizontal advection of angular momentum (divided by $\cos\varphi$), (c) vertical advection of angular momentum (divided by $\cos\varphi$), and (d) total circulation advection (sum of Plates 3b, 3c). Plates 3e-3h are for the perpetual January run.

Plate 3. Model angular momentum budget in seasonally varying run, showing the rate of change of zonal mean zonal wind due to (a) wave body force, (b) horizontal advection of angular momentum (divided by $\cos\varphi$), (c) vertical advection of angular momentum (divided by $\cos\varphi$), and (d) total circulation advection (sum of Plates 3b, 3c). Plates 3e-3h are for the perpetual January run.

Plate 4. Model zonal mean zonal wind $\overline{u}$, zonal mean meridional velocity $\overline{v}$, and zonal mean vertical velocity $\overline{w}$ in the perpetual January run of Experiment I.

Plate 4. Model zonal mean zonal wind $\overline{u}$, zonal mean meridional velocity $\overline{v}$, and zonal mean vertical velocity $\overline{w}$ in the perpetual January run of Experiment I.

Figure 3. Zonal mean vertical velocity at 15, 20, and 25 km.

Figure 3. Zonal mean vertical velocity at 15, 20, and 25 km.

Plate 5. (a, e): Perturbation $\overline{v}$ (top) and $\overline{w}$ (bottom) in Experiment I. (b, f): Same quantities but for Experiment II. (c, g): From Experiment III. (d, h): From Experiment IV.

Plate 5. (a, e): Perturbation $\overline{v}$ (top) and $\overline{w}$ (bottom) in Experiment I. (b, f): Same quantities but for Experiment II. (c, g): From Experiment III. (d, h): From Experiment IV.

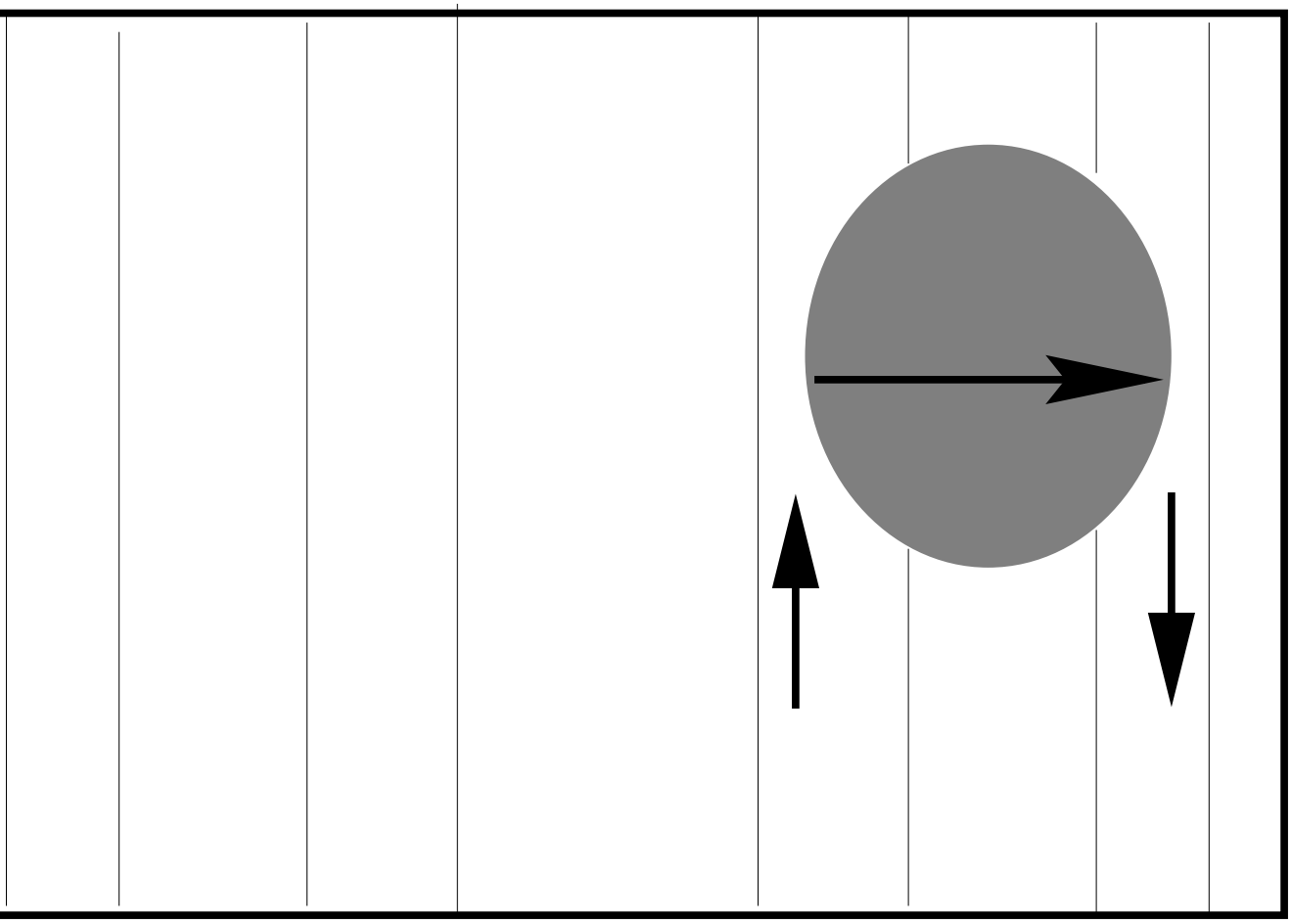

MMER
LE

EQ

WINTER
POLE

Figure 1

Anomaly in ozone column rate-of-change for Jan/Feb

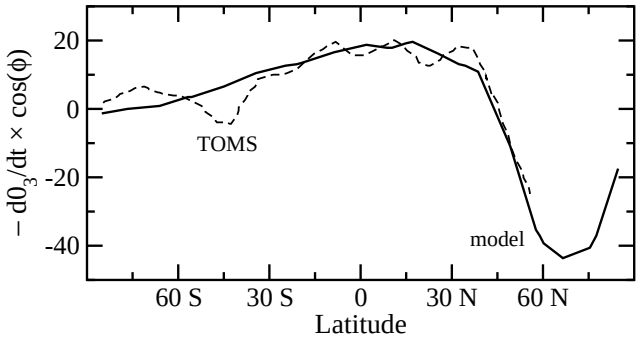

Figure 2

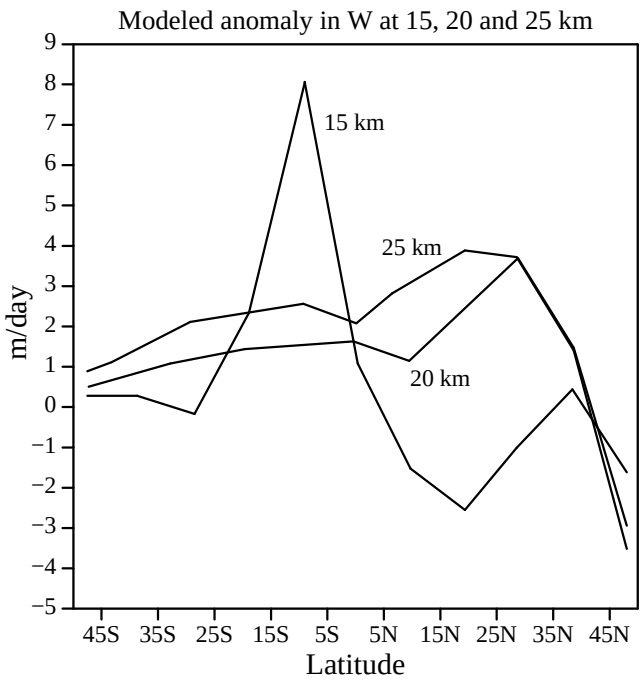
Modeled anomaly in W at 15, 20 and 25 km
m/day
9
8
7
6
5
4
3
2
1
0
−1
−2
−3
−4
−5
15 km
25 km
20 km
45S
35S
25S
15S
5S
5N
15N
25N
35N
45N
Latitude

Figure 3

(b)

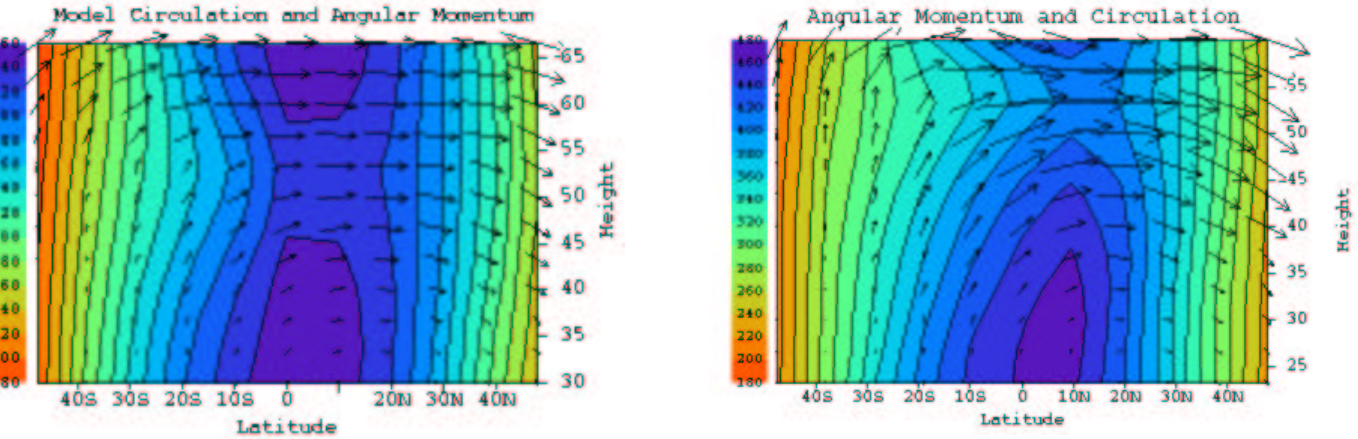
Model Circulation and Angular Momentum
Height
65
60
55
50
45
40
35
30
40S 30S 20S 10S 0 20N 30N 40N
Latitude
Angular Momentum and Circulation
Height
55
50
45
40
35
30
25
40S 30S 20S 10S 0 10N 20N 30N 40N
Latitude

Plate 1

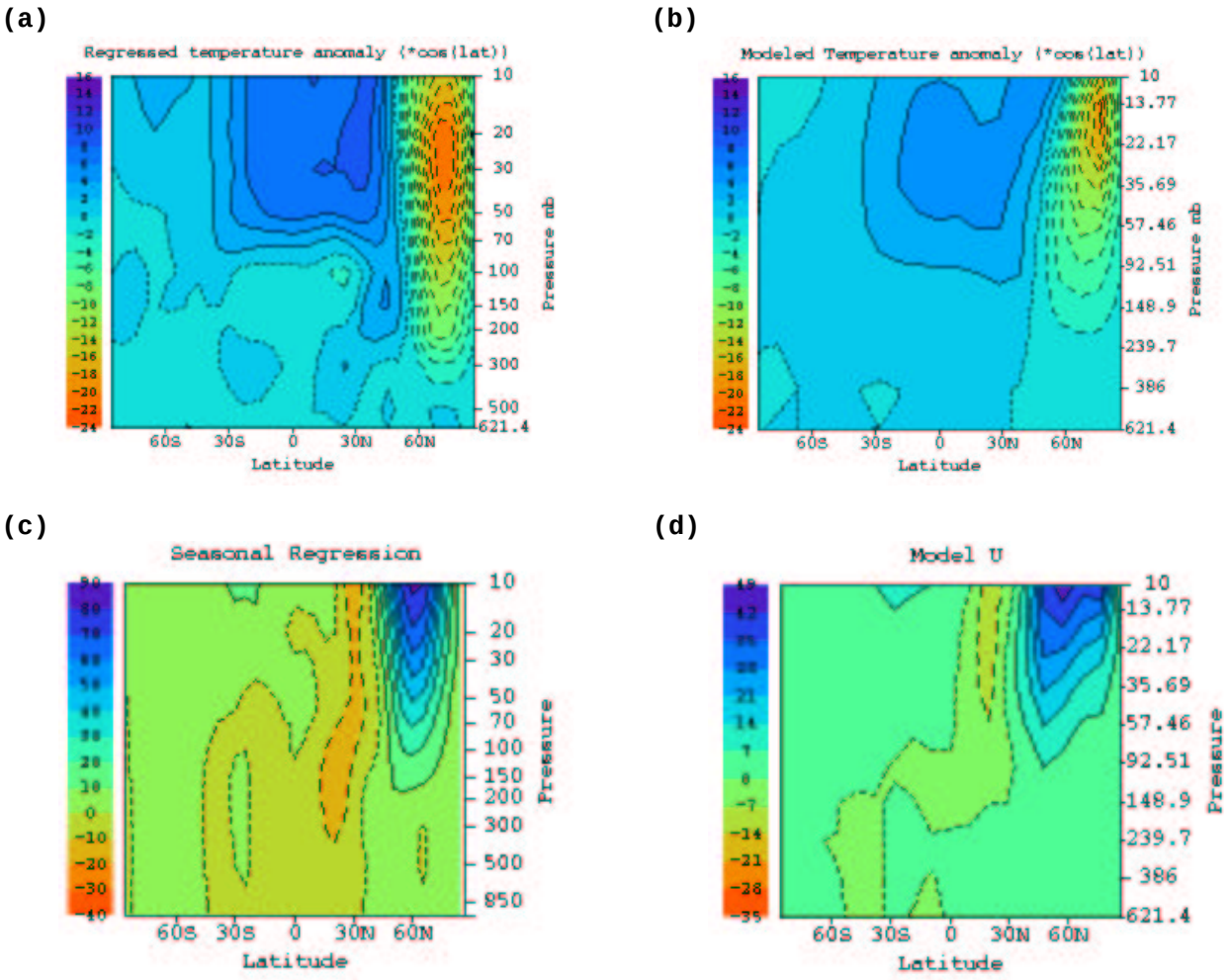
(a)
Regressed temperature anomaly (*cos(lat))
Pressure mb
Latitude
60S 30S 0 30N 60N
(b)
Modeled Temperature anomaly (*cos(lat))
Pressure mb
Latitude
60S 30S 0 30N 60N
(c)
Seasonal Regression
Pressure
Latitude
60S 30S 0 30N 60N
(d)
Model U
Pressure
Latitude
60S 30S 0 30N 60N

Plate 2

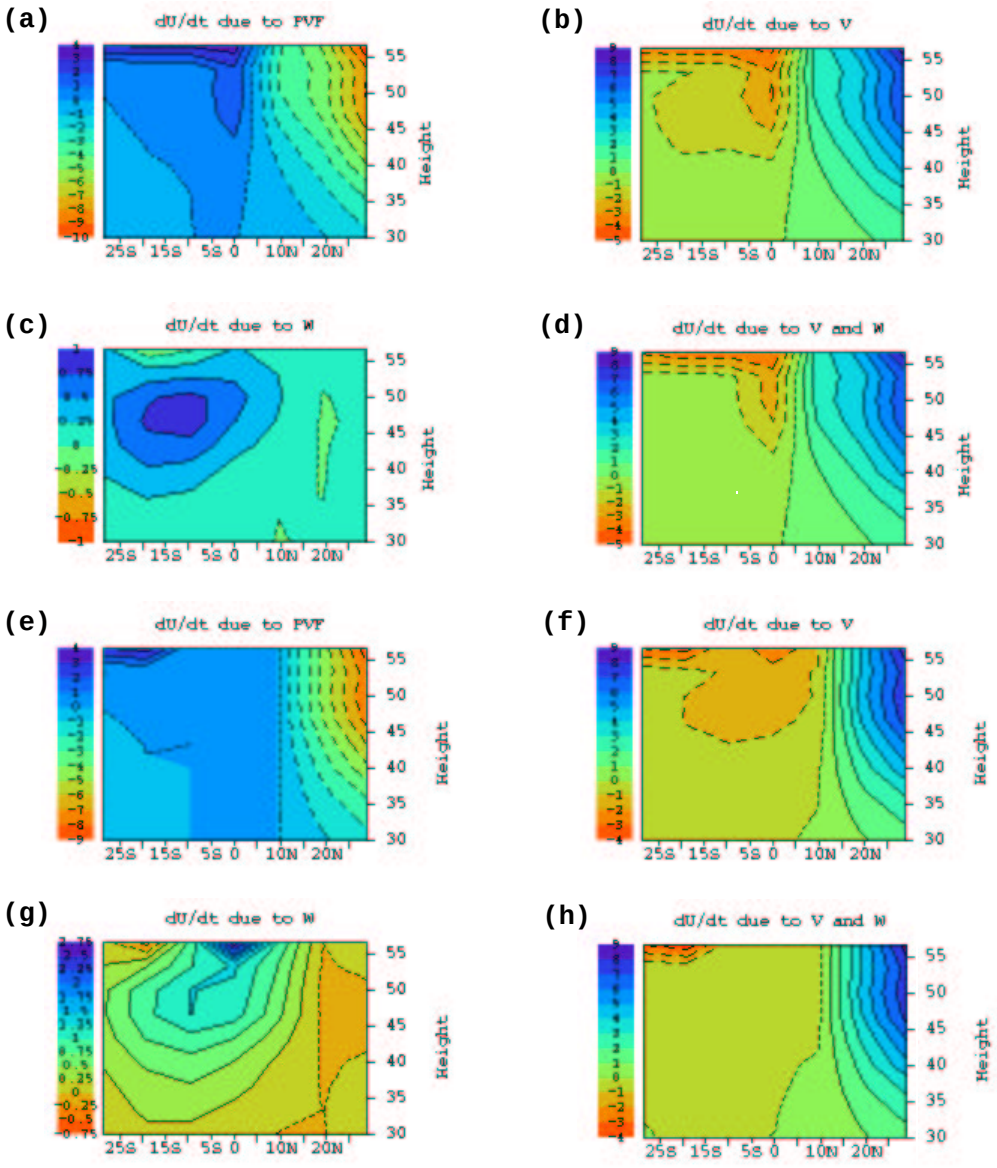
(a)
dU/dt due to PVF
(b)
dU/dt due to V
(c)
dU/dt due to W
(d)
dU/dt due to V and W
(e)
dU/dt due to PVF
(f)
dU/dt due to V
(g)
dU/dt due to W
(h)
dU/dt due to V and W
Height
55
50
45
40
35
30
25S 15S 5S 0 10N 20N

Plate 3

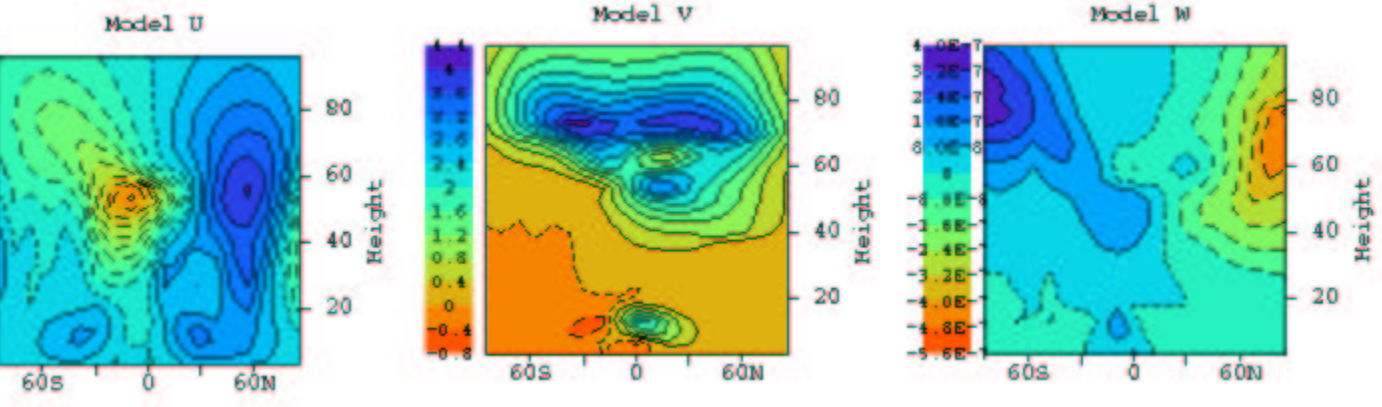

Plate 4

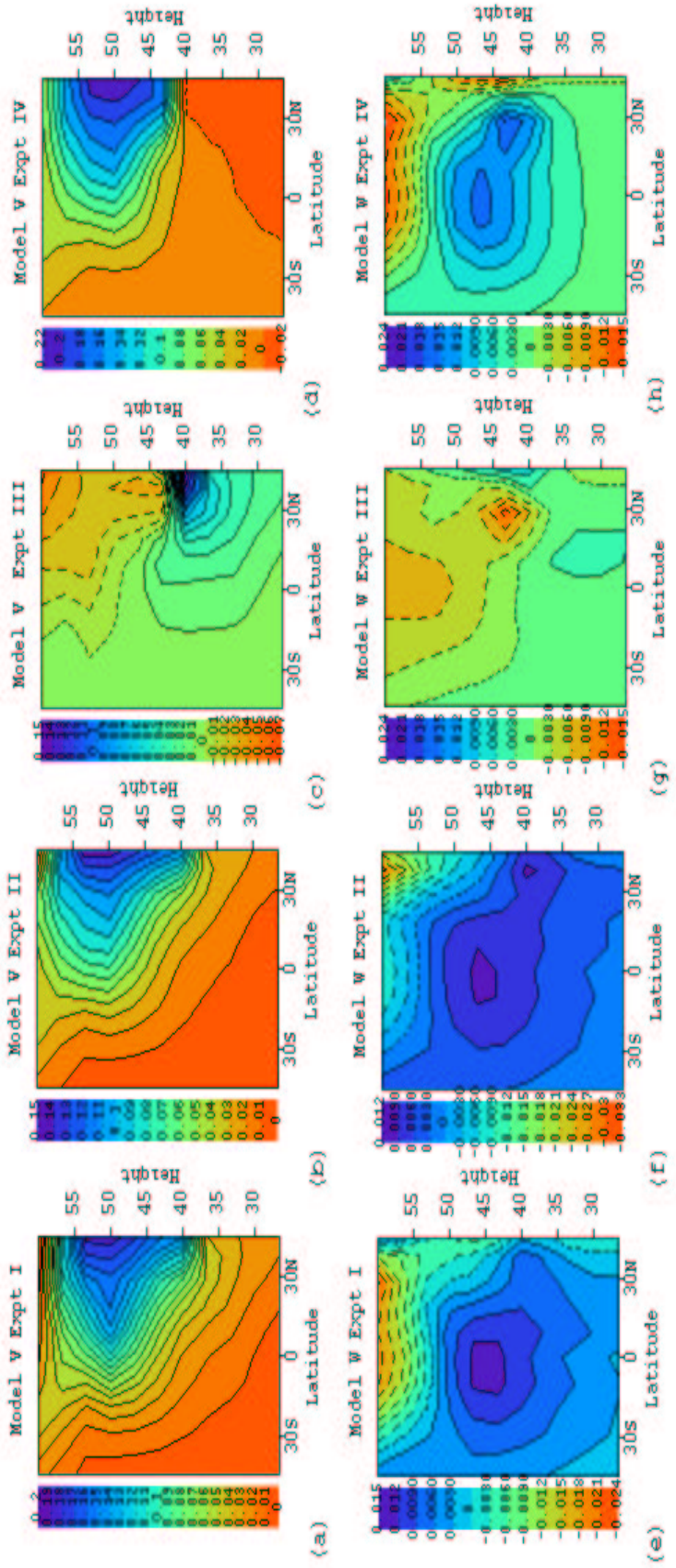
Model v Expt I
Model v Expt II
Model v Expt III
Model v Expt IV
Model w Expt I
Model w Expt II
Model w Expt III
Model w Expt IV
Height
Latitude
30S
0
30N
(a)
(b)
(c)
(d)
(e)
(f)
(g)
(h)

Plate 5

TUNG AND KINNERSLEY: CROSS-EQUATORIAL FLOW:

TUNG AND KINNERSLEY: CROSS-EQUATORIAL FLOW:

TUNG AND KINNERSLEY: CROSS-EQUATORIAL FLOW:

TUNG AND KINNERSLEY: CROSS-EQUATORIAL FLOW:

TUNG AND KINNERSLEY: CROSS-EQUATORIAL FLOW:

TUNG AND KINNERSLEY: CROSS-EQUATORIAL FLOW:

TUNG AND KINNERSLEY: CROSS-EQUATORIAL FLOW:

TUNG AND KINNERSLEY: CROSS-EQUATORIAL FLOW:

TUNG AND KINNERSLEY: CROSS-EQUATORIAL FLOW:

TUNG AND KINNERSLEY: CROSS-EQUATORIAL FLOW:

TUNG AND KINNERSLEY: CROSS-EQUATORIAL FLOW:

TUNG AND KINNERSLEY: CROSS-EQUATORIAL FLOW:

TUNG AND KINNERSLEY: CROSS-EQUATORIAL FLOW:

TUNG AND KINNERSLEY: CROSS-EQUATORIAL FLOW:

TUNG AND KINNERSLEY: CROSS-EQUATORIAL FLOW:

TUNG AND KINNERSLEY: CROSS-EQUATORIAL FLOW:

TUNG AND KINNERSLEY: CROSS-EQUATORIAL FLOW:

TUNG AND KINNERSLEY: CROSS-EQUATORIAL FLOW:

TUNG AND KINNERSLEY: CROSS-EQUATORIAL FLOW:

TUNG AND KINNERSLEY: CROSS-EQUATORIAL FLOW:

TUNG AND KINNERSLEY: CROSS-EQUATORIAL FLOW:

TUNG AND KINNERSLEY: CROSS-EQUATORIAL FLOW:

TUNG AND KINNERSLEY: CROSS-EQUATORIAL FLOW:

TUNG AND KINNERSLEY: CROSS-EQUATORIAL FLOW:

TUNG AND KINNERSLEY: CROSS-EQUATORIAL FLOW:

TUNG AND KINNERSLEY: CROSS-EQUATORIAL FLOW:

TUNG AND KINNERSLEY: CROSS-EQUATORIAL FLOW:

TUNG AND KINNERSLEY: CROSS-EQUATORIAL FLOW:

TUNG AND KINNERSLEY: CROSS-EQUATORIAL FLOW:

TUNG AND KINNERSLEY: CROSS-EQUATORIAL FLOW:

TUNG AND KINNERSLEY: CROSS-EQUATORIAL FLOW:

TUNG AND KINNERSLEY: CROSS-EQUATORIAL FLOW:

TUNG AND KINNERSLEY: CROSS-EQUATORIAL FLOW:

TUNG AND KINNERSLEY: CROSS-EQUATORIAL FLOW:

TUNG AND KINNERSLEY: CROSS-EQUATORIAL FLOW:

TUNG AND KINNERSLEY: CROSS-EQUATORIAL FLOW:

TUNG AND KINNERSLEY: CROSS-EQUATORIAL FLOW:

TUNG AND KINNERSLEY: CROSS-EQUATORIAL FLOW:

TUNG AND KINNERSLEY: CROSS-EQUATORIAL FLOW:

TUNG AND KINNERSLEY: CROSS-EQUATORIAL FLOW:

TUNG AND KINNERSLEY: CROSS-EQUATORIAL FLOW:

TUNG AND KINNERSLEY: CROSS-EQUATORIAL FLOW:

TUNG AND KINNERSLEY: CROSS-EQUATORIAL FLOW:

TUNG AND KINNERSLEY: CROSS-EQUATORIAL FLOW:

TUNG AND KINNERSLEY: CROSS-EQUATORIAL FLOW:

TUNG AND KINNERSLEY: CROSS-EQUATORIAL FLOW:

TUNG AND KINNERSLEY: CROSS-EQUATORIAL FLOW:

TUNG AND KINNERSLEY: CROSS-EQUATORIAL FLOW:

TUNG AND KINNERSLEY: CROSS-EQUATORIAL FLOW:

TUNG AND KINNERSLEY: CROSS-EQUATORIAL FLOW:

TUNG AND KINNERSLEY: CROSS-EQUATORIAL FLOW:

TUNG AND KINNERSLEY: CROSS-EQUATORIAL FLOW:

TUNG AND KINNERSLEY: CROSS-EQUATORIAL FLOW:

TUNG AND KINNERSLEY: CROSS-EQUATORIAL FLOW:

TUNG AND KINNERSLEY: CROSS-EQUATORIAL FLOW: